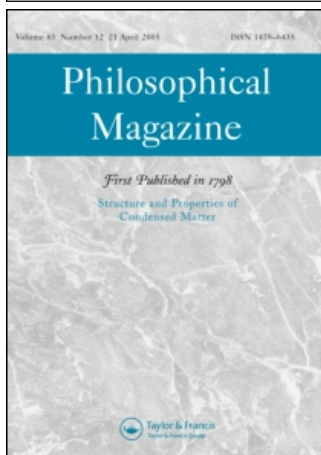


This article was downloaded by:[Los Alamos National Laboratory]
On: 27 November 2007
Access Details: [subscription number 768609635]
Publisher: Taylor & Francis
Informa Ltd Registered in England and Wales Registered Number: 1072954
Registered office: Mortimer House, 37-41 Mortimer Street, London W1T 3JH, UK



Philosophical Magazine

First published in 1798

Publication details, including instructions for authors and subscription information:
<http://www.informaworld.com/smpp/title~content=t713695589>

Microstructure of Ag/BaTiO₃ films grown on MgO(100) substrate under external electric field

M. J. Zhuo^{ab}; X. L. Ma^a

^a Shenyang National Laboratory for Materials Science, Institute of Metal Research, Chinese Academy of Sciences, 110016 Shenyang, China

^b Graduate School of Chinese Academy of Sciences, 100049 Beijing, China

Online Publication Date: 01 November 2007

To cite this Article: Zhuo, M. J. and Ma, X. L. (2007) 'Microstructure of Ag/BaTiO₃ films grown on MgO(100) substrate under external electric field', Philosophical Magazine, 87:32, 5117 - 5128

To link to this article: DOI: 10.1080/14786430701618480

URL: <http://dx.doi.org/10.1080/14786430701618480>

PLEASE SCROLL DOWN FOR ARTICLE

Full terms and conditions of use: <http://www.informaworld.com/terms-and-conditions-of-access.pdf>

This article maybe used for research, teaching and private study purposes. Any substantial or systematic reproduction, re-distribution, re-selling, loan or sub-licensing, systematic supply or distribution in any form to anyone is expressly forbidden.

The publisher does not give any warranty express or implied or make any representation that the contents will be complete or accurate or up to date. The accuracy of any instructions, formulae and drug doses should be independently verified with primary sources. The publisher shall not be liable for any loss, actions, claims, proceedings, demand or costs or damages whatsoever or howsoever caused arising directly or indirectly in connection with or arising out of the use of this material.

Microstructure of Ag/BaTiO₃ films grown on MgO(100) substrate under external electric field

M. J. ZHUO^{†‡} and X. L. MA^{*†}

[†]Shenyang National Laboratory for Materials Science, Institute of Metal Research,
Chinese Academy of Sciences, 110016 Shenyang, China

[‡]Graduate School of Chinese Academy of Sciences, 100049 Beijing, China

(Received 12 February 2007; accepted in revised form 7 August 2007)

By applying an electric field parallel to the substrate surface, highly ordered Ag nanoparticles were homogeneously embedded in BaTiO₃ (BTO) films grown on a MgO(100) substrate. Transmission electron microscopy studies show that the BTO film is [100]-oriented. The general crystallographic orientation relationships between the composite film and MgO substrate are [100]_{BTO}//[100]_{Ag}//[100]_{MgO} and (010)_{BTO}/(010)_{Ag}/(010)_{MgO}. However, in films grown without an external electric field, Ag particles grow with random orientations and the BTO matrix is polycrystalline. Thus, electric fields are thought to meliorate the quality of the films by changing the growth orientation. In addition, the BTO matrix and Ag particles were found to be multiply twinned from studies on cross-sectional specimens. The contribution is discussed of Ag particles with ordered growth orientation and the large amount of BTO microtwins with higher dielectric constant to the improved optical properties of the as-prepared composite films.

1. Introduction

Metal nanoparticles either dispersed in a dielectric matrix or attached on surfaces of a metal oxide have been extensively studied. Metallic nanoclusters dispersed in a dielectric material have been found to affect its optical, magnetic and electrical properties [1]. For instance, the system of gold nanoclusters dispersed in TiO₂ surface displays a high activity for low temperature oxidation of CO to CO₂ [2, 3] and a high sensitivity as a low temperature CO gas sensor [2]. During the past few years, semiconductor and metallic nanoparticles have been dispersed into a variety of host materials by different preparation methods, such as sol-gel [4], ion implantation [5], pulsed-laser deposition (PLD) [6] and radio-frequency co-sputtering [7]. In these systems, metal particles include Ag, Au, Sn, Cu, Zn, Fe, Mn, Ni, Cr and Pb, and the dielectric matrices include SiO₂, MgF₂, Al₂O₃, BaTiO₃ (BTO), SrTiO₃, etc.

Composite films of noble metal nanoparticles embedded in a dielectric medium have been reported to display desirable optical properties [1, 4, 7–9]. Due to the large third order nonlinear susceptibility ($\chi^{(3)}$) at the special surface plasmon resonance (SPR) frequency, these nanocomposites films have received increasing attention and

*Corresponding author. Email: xлма@imr.ac.cn

have great potential for applications in areas such as nonlinear optical devices and fast optical switching devices. The large $\chi^{(3)}$ has been found to be dependent on the local field enhancement near the SPR of metal particles. Thus, metal particles (e.g. Ag, Au and Cu) with strong plasmon resonance and the matrices with high dielectric constant, large nonlinear optical effect, and ferroelectricity (e.g. BTO, LiNbO₃) have been proposed as special kinds of candidates. In this work, Ag/BTO composites were investigated. Generally, it was recognized that the physical properties of the films are strongly sensitive to the quality of the microstructural features of composite films, such as the distribution, size, shape of the metal particles and the crystallization of the surrounding medium, which are controlled by the preparation conditions [5–7, 9–13]. Haus *et al.* [14] reported that the nonlinearity can be enhanced by using non-spherical (e.g. ellipsoidal) particles. They also presented the results of higher nonlinearity for oriented particles by comparing with random configuration of the particles. For the composite system, theoretically, Yuen *et al.* [15] and Wen *et al.* [16] recently revealed that the geometric anisotropy in nonlinear thin films greatly enhanced the optical nonlinearity. Experimentally, Guan *et al.* [17] observed a significant enhancement of optical nonlinearity in Ag/BTO composite films prepared under an applied electric field during the growth process.

Electric or magnetic fields have been widely used during the film deposition process to tune the properties of films [18–25]. Owing to the special oriented structure induced by the external applied fields, films exhibit enhanced properties. However, most of structural characterizations have been carried out by X-ray diffraction, scanning electron microscopy and atomic force microscopy. There are few reports on transmission electron microscopy (TEM) studies of these films, especially for the geometric anisotropy in the structure. In this work, we present, by means of extensive TEM studies, the microstructure characteristics of the composite Ag/BTO film grown under an external electric field. The influence of the applied electric field on the orientation ordering of the composite films and the contribution of the microstructures to the enhanced properties are discussed.

2. Experimental procedures

Ag/BTO films with a thickness about 150 nm were grown on the MgO(100) substrate using a pulsed-laser deposition method. A Xe–Cl excimer laser (308 nm, 17 ns, 4 Hz) was used as the laser source. Several fan-shaped chips of 99.99% pure Ag were uniformly placed on the surface of the BTO target, and the ratio between the Ag area and the target area was 1:8. The target was mounted on a rotation holder, 40 mm away from the MgO substrate. The films were deposited in an N₂ atmosphere with pressure of 10.0 Pa. The substrate was maintained at 600°C during the entire deposition process. An electric field was applied parallel to the surface and along the $\langle 100 \rangle$ direction of the substrate, the distance between the two electrodes was 2 cm. The samples were grown with external voltage of 2000 V and 0 V, which were not switched off until the films were cooled down to room temperature. Thin foils for TEM investigations were prepared by conventional methods consisting of slicing, grinding, dimpling and finally ion milling. Electron diffraction and TEM images of

the as-received films were performed on a JEOL 2010 with a point resolution of 0.194 nm. A Tecnai G² F30 TEM, which was equipped with a high-angle annular dark field (HAADF) detector and an energy dispersive spectroscopy (EDS) system, was used for the high-resolution Z-contrast images and compositional analysis.

3. Experimental results

3.1. Microstructures of Ag/BTO films grown with external electric field

3.1.1. Plan-view observations. Figure 1a is a low-magnification plan-view HAADF image of the Ag/BTO films grown under an external electric field. The most salient feature is that rectangular nanoparticles, about 50 nm in size, are homogeneously distributed in the BTO medium. In addition, many much smaller nanoparticles, also with white contrast, are dispersed around the rectangular particles. Figure 1b is a corresponding composite electron diffraction pattern (EDP) of figure 1a, which covers both Ag/BTO film and MgO substrate. The very weak diffraction rings seen in figure 1b indicate that the film medium is not single crystallized.

The following further analyses will illustrate the microstructures. Figure 2 displays EDS area-scanning maps showing the elemental distribution in the film matrix and the particles. It reveals that the particles are rich in Ag and poor in Ba and Ti, whereas the film matrix exhibits opposite features. It is also clear that the small dots between the larger particles display the same compositional characteristics as the larger particles. Nanobeam diffraction (NBD) analyses upon variant nanoparticles indicate that they are pure Ag. A typical NBD pattern of Ag [100] zone axis is shown in figure 3. In other words, the white-contrast particles in figure 1a are single crystalline Ag, which is in accord with the previous XPS result [17].

Based on the above results, more information can be deduced from the composite EDP presented in figure 1b. It is clear that the diffraction spots with high indexes split, such as those denoted by arrows. An enlarged view of the splitting

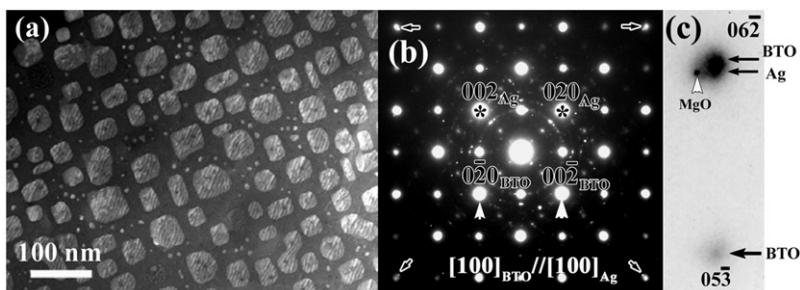


Figure 1. (a) A low-magnification plan-view HAADF image of Ag/BTO composite film grown with external electric field. (b) Corresponding selected area electron diffraction pattern of (a). (c) An enlarged view of the splitting diffraction spots of high indexes.

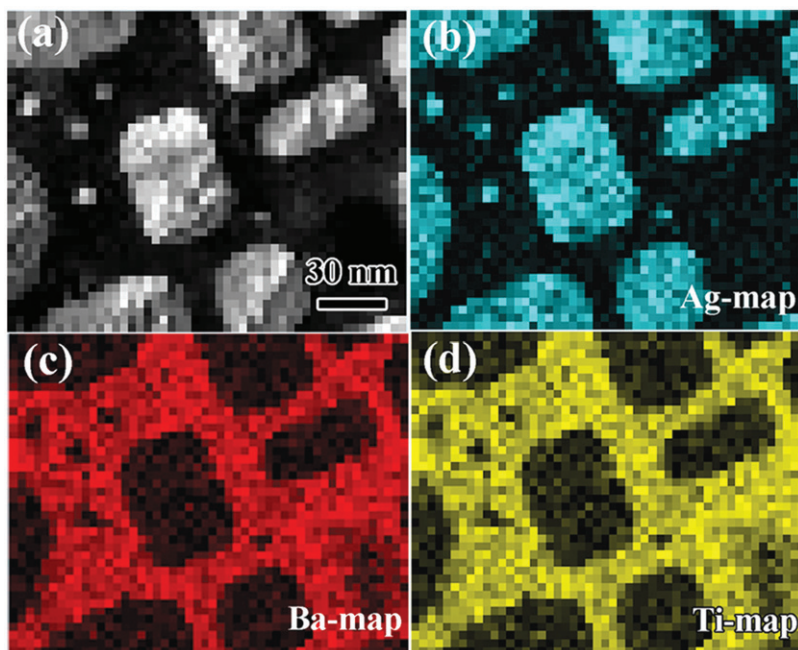


Figure 2. (a) A low-magnification plan-view image. (b)–(d) EDS elemental maps showing the distribution of Ag, Ba and Ti, respectively. The four images have the same scale bar.

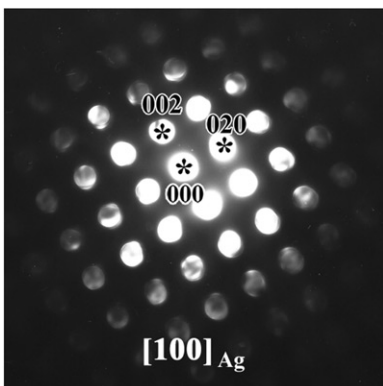


Figure 3. NBD pattern taken from an Ag particle along the $[001]$ zone axis showing that the Ag particle is single crystal.

diffraction spots is shown in figure 1c. Ignoring sporadic diffraction spots, the outer splitting diffraction spots are not only produced by the tetrahedral BTO but also yielded by Ag particles due to their slightly different lattice parameters: the lattice parameter of cubic Ag is about 0.408 nm and BTO has a tetrahedral structure with lattice parameters of $a=b=0.3995$ nm and $c=0.4038$ nm. The inner splitting spots

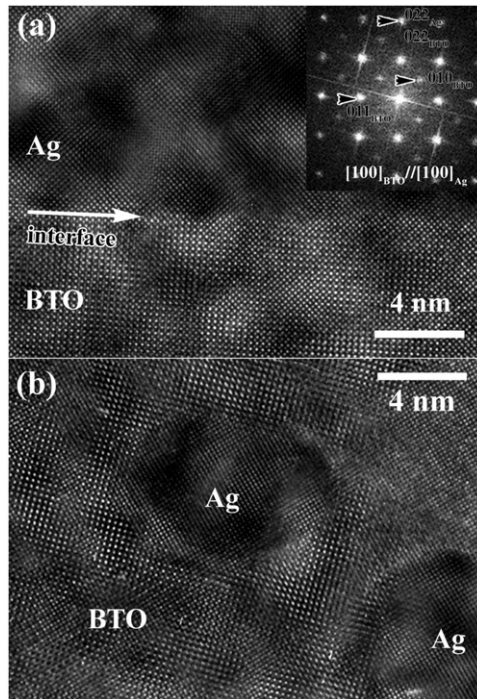


Figure 4. (a) HREM image shows the atomic structure across the Ag/BTO interface. The inset is the corresponding FFT image, which shows the orientation relationship of $[100]_{\text{BTO}}/[100]_{\text{Ag}}$, $(010)_{\text{BTO}}/(010)_{\text{Ag}}$ between the Ag particles and the BTO matrix. (b) HREM image showing the atomic structure between the smaller Ag particle and BTO matrix.

can be indexed as the $[100]$ zone axis of cubic MgO, the lattice parameter of which is about 0.421 nm. As a result, the orientation relationships of $[100]_{\text{BTO}}/[100]_{\text{MgO}}/[100]_{\text{Ag}}$ and $(010)_{\text{BTO}}/(010)_{\text{MgO}}/(010)_{\text{Ag}}$ can be derived.

Figure 4a shows a high-resolution electron microscopic (HREM) image showing the interface of an Ag particle and BTO medium in a plan-view specimen. The inserted image in figure 4a is the corresponding fast Fourier transformation (FFT) image across the Ag/BTO interface, confirming that Ag particles satisfy the orientation relationship of $[100]_{\text{BTO}}/[100]_{\text{Ag}}$, $(010)_{\text{BTO}}/(010)_{\text{Ag}}$ with respect to BTO film. Another feature is that Ag particles share a coherent interface with the BTO matrices, which agree well with the low lattice misfit between Ag and BTO. Figure 4b shows an HREM image including smaller Ag particles, confirming that these particles follow the similar growth orientation and Ag/BTO relationship as the larger silver particles.

3.1.2 Cross-sectional observations. In order to obtain more details on the microstructure of Ag particles and BTO film, cross-sectional specimens were prepared and investigated. Figure 5a shows a low-magnification cross-sectional HAADF image of the Ag/BTO films viewed nearly along the $\langle 110 \rangle$ direction of the MgO substrate. The shape of the Ag particles with white contrast is not as regular as

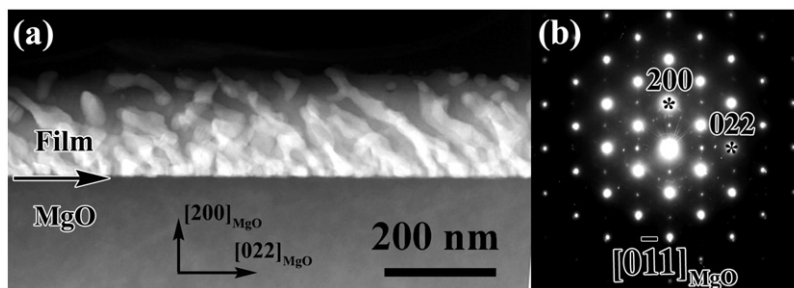


Figure 5. (a) A low-magnification cross-sectional HAADF image. (b) Corresponding selected area electron diffraction patterns taken along the MgO[011] direction. The (022) and (200) diffraction spots were indexed.

that shown in plan-view image. Also, the Ag particles incline to the $[0\bar{1}1]$ direction in the image. That is, the conglomeration direction of the particles was induced by the external applied field that was parallel to the $\langle 100 \rangle$ direction of the MgO substrate. The corresponding EDP is shown in figure 5b, also exhibiting the sporadic diffraction spots.

Figure 6a shows an HREM image across the composite film/MgO interface including an Ag particle. The continuous lattice across the BTO/MgO, Ag/MgO and Ag/BTO interfaces confirm the growth orientation among the BTO, Ag and MgO substrate. The upright Ag/BTO boundary turns left, indicating the irregular shape of Ag particles. In addition, twin structure, the $\{111\}$ boundaries of which are marked by black arrows, was observed in BTO region. Furthermore, the microtwins of BTO are most common near the BTO/MgO interface. As shown in figure 6b, a large amount of microtwins overlap one another. The inset in figure 6b is the corresponding FFT image. The apparent diffraction spots from BTO twins and streaking lines along different $\langle 111 \rangle$ directions in the FFT pattern are observed. Both HREM image and the FFT pattern revealed the presence of microtwins in BTO medium. These microtwins are found to originate from the interface, as shown in areas A, B, C and D in figure 6b, which can effectively relax the interface strain arise from the lattice mismatch. No misfit dislocations are observed at the interface between the film and the substrate, so a mechanism of stress induction of twins by lattice mismatch is suggested. Figures 6c and 6d display high-resolution HAADF images of nanotwin lamellae. Figure 6d is the FFT filtered image of figure 6c, showing five ordered nanotwin lamellae. The numbers “23233” denote the numbers of $\{111\}$ planes between the neighbouring $\{111\}$ twin planes. Of course, if the number decreases, a planar fault would form. Moreover, because the contrast of HAADF images is nearly proportional to the square of atomic number, the higher intensity of atom columns at the twin boundaries indicates that the twin planes are BaO–O planes. On the other hand, twins also form in the Ag particles because of the lower formation energy.

Figure 7 shows Ag twins with two types of $\{111\}$ twin planes denoted by T1 and T2. The inserted images are corresponding FFT patterns of Ag(110) zone, showing clear twin diffraction spots. The streaking lines in the T2 FFT pattern presents that except for the nanotwins, planar faults also cannot be excluded. Due to the existence

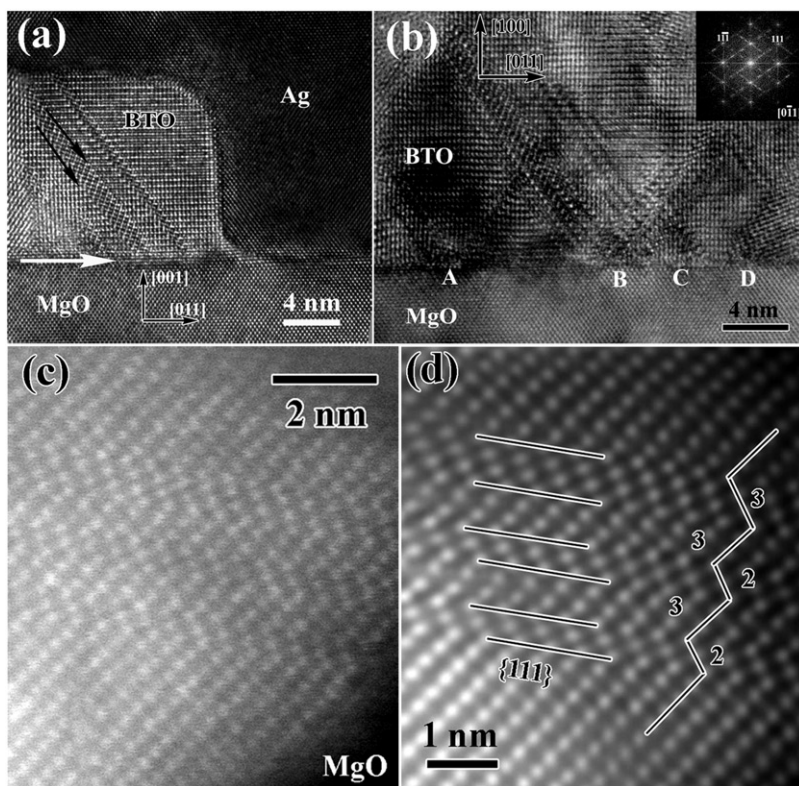


Figure 6. (a) Cross-sectional HREM image viewed along the $\text{MgO}[0\bar{1}1]$ direction. (b) HREM image showing the microtwins in the BTO matrix near BTO/MgO interface. (c) High-resolution HAADF image showing the ordered multiple nanotwin lamellae. (d) FFT filtered image of (c). The numbers “23233” denote the numbers of $\{111\}$ planes between the neighbouring $\{111\}$ twin planes.

of Ag particles, most BTO microtwins terminate inside the film and cannot extend to the film surface. In such a composite film with diverse microstructure, the beam was diffracted and deflected not only by different phase but also by various defects, so that sporadic diffraction spots appear (figures 1b and 5b) and diverse moiré fringes are observed (figure 1a).

3.2. Investigations of Ag/BTO films grown without external electric field

Figure 8a shows a low-magnification plan-view HAADF image of a Ag/BTO composite film grown without an external field. The Ag particles with white contrast exhibit round morphology, which is different from that in figure 1a. But the particles show the same chemical composition, which is not shown for brevity, to that in figure 2. Figure 8b is the EDP recorded from the plan-view specimen covering the composite films and MgO substrate. Due to the larger lattice constants of MgO than BTO and Ag, apparent diffraction spot splitting with high indexes are also observed, similar to that in figures 1b and 1c. It is worth noting that the outer splitting

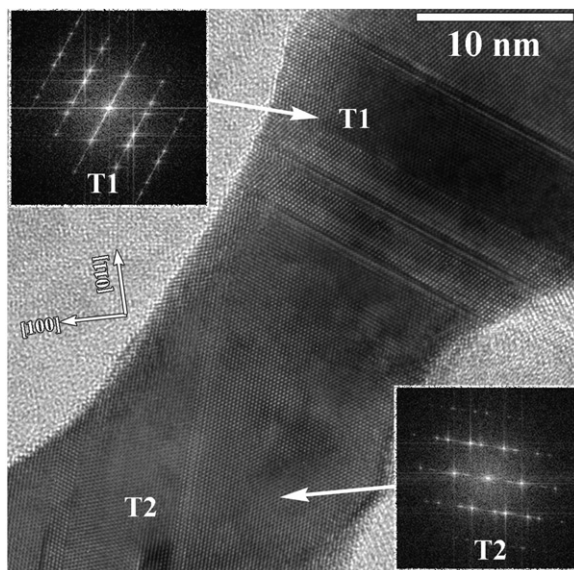


Figure 7. Twin structures (T1 and T2) with different $\{111\}$ twin plane in Ag particle. The insets are the corresponding FFT patterns.

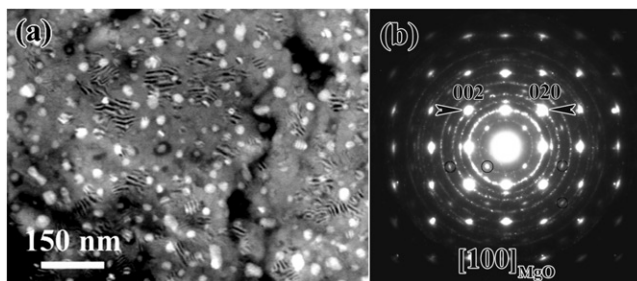


Figure 8. (a) A low-magnification plan-view HAADF images of a Ag/BTO composite film without external field. (b) Composite EDP taken from plan-view specimen along MgO[100] direction.

diffraction spots are elongated along the arc direction and weak diffraction rings are formed. Moreover, diffraction spots of $\{0n0\}_{\text{BTO}}$ with odd n produced only by BTO, such as those denoted by black open circles, are obvious, but they also exhibit very weak diffraction rings. As a result, it can be concluded that the BTO has a structure of polycrystalline texture, which is different from the structures of those grown on SrTiO_3 by PLD with different conditions, for they have highly epitaxial BTO films [26, 27]. Apart from the aforementioned weak rings, the clear diffraction rings should involve those from Ag particles, which overlap those from BTO because of the similar lattice constants. Therefore, it appears that Ag particles grow with random directions. Due to the polycrystalline structure, the twin structure and the cross-sectional views are not shown for brevity.

4. Discussions

4.1. Growth mechanism for Ag particles with ordered orientation

Compared to films grown without an external field, the composite films deposited under an external electric field are highly ordered with [100] growth orientation. Esteban and Rojo [28], Murayama [19] and Chopra [18] have studied the influence of electric field on the growth orientation of metal films. Gold or silver films change from polycrystalline to (001) orientation with the help of an electric field. The enhanced orientation effects are thought to have a close relationship with the film formation processes of nucleation and coalescence. Pashley *et al.* [29] pointed out that the change from a partially oriented to a perfectly epitaxial film induced by external field was due to the reorientation and recrystallization of nuclei during coalescence. The detail description about the influence of the electric field on the coalescence stage was explained in terms of electrostatic charge effects [18]. Thus, with the help of an external electric field, the Ag particles in the as-received film prefer to grow with [100] direction. Meanwhile, the free energy of Ag particles increases due to the electrostatic charge effects. In order to consume the increased energy induced by external field, the original spherical silver particles become prolate. The final shapes of the particles are determined by the balance of the total energy. Similarly, the imposed field-induced enhanced orientation effects can also improve the growth orientation of BTO matrix. That is why more intense and sharp diffraction spots were observed in film with the external field, as shown in figure 1b and figure 8b. When the films were cooled to a temperature below T_c , at which paraelectric BTO is transformed to ferroelectric, under electric field forces its polarized direction (the [001] direction of tetrahedral BTO) would turn to the direction parallel to the applied electric field. Generally, in this way, BTO film matrices have a preferential [100]-orientation instead of [001]-orientation. The crystallographic orientation relationship described as $[100]_{\text{BTO}}//[100]_{\text{Ag}}, (010)_{\text{BTO}}// (010)_{\text{Ag}}$ is formed. Actually, because of the large BTO/MgO lattice misfit of about 4.88%, lots of microtwins form near the film/substrate interface to relieve the lattice mismatch-induced strain.

4.2. Microstructure–property relationship

Optical properties in Ag/BTO composite films with or without external electric field have been studied by Guan *et al.* [17]. It was demonstrated that an external field can enhance the optical nonlinearity of the metal–dielectric composite films greatly. The improved optical properties can be explained based on the observed microstructures. When Ag particles are oriented parallel to one another, the effective dielectric medium will be anisotropic. With the textured BTO matrix, the local electric field inside the metal particles is enhanced [14]. Hence, the depolarization tensor that depends on the non-spherical shape of the particles also affects the magnitude of the local field in the particles. Thus, the highly ordered orientation of metal particles with non-spherical shapes in the films contributes significantly to the large enhancement of the optical nonlinearity of Ag/BTO films.

Besides the interesting and specific growth orientation, microtwins in the BTO matrix are also imputed to enhance optical properties. In the cubic and tetragonal

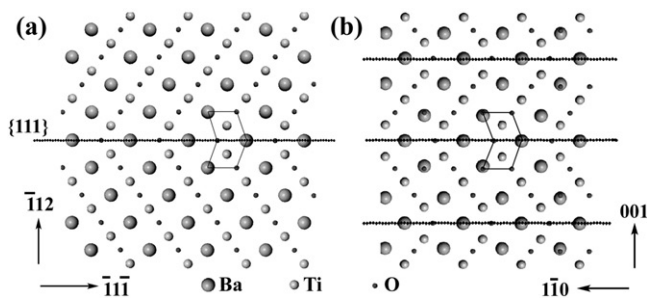


Figure 9. Schematic perspective of (a) cubic BTO $\{111\}$ twin in a $[110]$ projection, and (b) hexagonal BTO in a $[110]$ projection, showing that BTO $\{111\}$ twin have the same structure unit in hexagonal BTO as marked by rhombuses.

BTO structure, the oxygen octahedra in the $\{111\}$ twin planes are coplanar, as shown in figure 9a. According to the contrast of twin planes in figures 6c and 6d, figure 9a shows the twin plane with BaO–O. In hexagonal BTO, the oxygen octahedra share the face instead of the corner as found in the perfect cubic and tetragonal structure, as shown in figure 9b. The coplanar oxygen octahedra, marked by rhombuses in figure 9, indicate that the atoms near the twin boundary exhibit similar arrangement as some part of the hexagonal unit cell [30, 31]. So, the appearance of these twins can be attributed to the existence of a hexagonal structure modification in the BTO compound. If the multiple nanotwin lamellae were ordered, as shown in figures 6c and 6d, they would result in a structure similar to the hexagonal phase. With respect to the hexagonal BTO, Yu *et al.* [32] have reported that oxygen-deficient hexagonal BTO exhibits a dielectric constant higher than 100 000 with a loss component of about 0.1 together with a weak temperature dependence in the range of 100 to 300 K. However, in the twin structure of BTO, Jia and Urban [33] measured the oxygen concentration at the BTO twin boundaries and show that only 68% oxygen sites are occupied. That is, multitwins with lots of boundaries are oxygen-deficient. As a consequence, the BTO with a lot of microtwins (or say oxygen-deficient hexagonal structure units) may have a higher dielectric constant compared with the perfect tetragonal BTO.

In such metal–ceramic composites, the third-order optical nonlinear susceptibility values increase when the local field around the metal particle is enhanced by the optical excitation of a surface plasmon in the metal particle. The local field enhancement also strongly depends on the dielectric constant and refractive index of the matrix of the metal-dispersed thin film. That is, the $\chi^{(3)}$ is proportional to the dielectric constant of the matrix. As a consequence, the microtwin structure may contribute to an improvement of the optical properties.

5. Conclusions

In summary, microstructures of Ag/BaTiO₃ films deposited on the MgO (001) substrate under different external electric field have been investigated by various TEM techniques. The films grown without external electric field were observed to be

polycrystalline and the Ag particles are spherical. When an external electric field was applied, an ordering orientation of Ag nanoparticles in crystalline BTO was revealed. These Ag particles are about 50 nm in dimension and followed a unique orientation relationship with the BTO matrix and MgO substrate: $[100]_{\text{BTO}}//[100]_{\text{Ag}}//[100]_{\text{MgO}}$, and $(010)_{\text{BTO}}//[(010)_{\text{Ag}}//[(010)_{\text{MgO}}$. Moreover, high-density microtwins in the BTO matrix were observed, which were thought to improve the dielectric constant of BTO. The uniform Ag particles distribution with specific growth orientation and microtwins with higher dielectric constant play a key role in improving the third-order optical nonlinear susceptibility values.

Acknowledgments

We would like to thank Professor H. B. Lu, Institute of Physics, Chinese Academy of Sciences, for providing the samples. This work was supported by the National Natural Science Foundation of China with Grant No. 50325101 and Special Funds for the Major State Basic Research Projects of China (Grant No. 2002CB613503).

References

- [1] D.M. Sun and Z.Q. Sun, *Metal-Ceramic Films and their Applications in Optic-Electric Techniques* (Science Publishing Press, Beijing, 2004), (in Chinese).
- [2] F. Cosandey and T.E. Madey, *Surf. Rev. Lett.* **8** 73 (2001).
- [3] M. Valden, X. Lai and D.W. Goodman, *Science* **281** 1647 (1998).
- [4] S. Otsuki, K. Nishio, T. Kineri, *et al.*, *J. Am. Ceram. Soc.* **82** 1676 (1999).
- [5] Z.X. Liu, H. Li, X.D. Feng, *et al.*, *J. Appl. Phys.* **84** 1913 (1998).
- [6] G. Yang, W.T. Wang, Y.L. Zhou, *et al.*, *Appl. Phys. Lett.* **81** 3969 (2002).
- [7] B. Wang and L.D. Zhang, *Appl. Surf. Sci.* **133** 152 (1998).
- [8] U. Kreibig and L. Genzel, *Surf. Sci.* **156** 678 (1985).
- [9] F. Hache, D. Ricard and C. Flytzanis, *J. Opt. Soc. Am. B* **3** 1647 (1986).
- [10] A.A. Scalisi, G. Compagnini, L. D'Urso, *et al.*, *Appl. Surf. Sci.* **226** 237 (2004).
- [11] R. del Coso, J. Requejo-Isidro, J. Solis, *et al.*, *J. Appl. Phys.* **95** 2755 (2004).
- [12] W.T. Wang, G. Yang, Z.H. Chen, *et al.*, *J. Appl. Phys.* **92** 7242 (2002).
- [13] S. Debrus, J. Lafait, M. May, *et al.*, *J. Appl. Phys.* **88** 4469 (2000).
- [14] J.W. Haus, R. Inguva and C.M. Bowden, *Phys. Rev. A* **40** 5729 (1989).
- [15] K.P. Yuen, M.F. Law, K.W. Yu, *et al.*, *Phys. Rev. E* **56** R1322 (1997).
- [16] W.J. Wen, N. Wang, H.R. Ma, *et al.*, *Phys. Rev. Lett.* **82** 4248 (1999).
- [17] D.Y. Guan, Z.H. Chen, W.T. Wang, *et al.*, *J. Opt. Soc. Am. B* **22** 1949 (2005).
- [18] K.L. Chopra, *J. Appl. Phys.* **37** 2249 (1966).
- [19] Y. Murayama, *Thin Solid Films* **12** 287 (1972).
- [20] O. Vigil, Y. Rodriguez, O. Zelaya-Angel, *et al.*, *Thin Solid Films* **322** 329 (1998).
- [21] W.P. Hu, Y.Q. Liu, S.Q. Zhou, *et al.*, *Thin Solid Films* **347** 299 (1999).
- [22] Z.G. Ji, K.W. Wong, P.K. Tse, *et al.*, *Thin Solid Films* **402** 79 (2002).
- [23] J. Vidal, O. de Melo, O. Vigil, *et al.*, *Thin Solid Films* **419** 118 (2002).
- [24] B. Alterkop, N. Parkansky, R.L. Boxman, *et al.*, *Thin Solid Films* **290** 10 (1996).
- [25] D.J. Bergman and Y.M. Strelniker, *Phys. Rev. Lett.* **80** 857 (1998).

- [26] J. Hiltunen, D. Seneviratne, R. Sun, *et al.*, Appl. Phys. Lett. **89** 242904 (2006).
- [27] J. Zhang, D.F. Cui, H.B. Lu, *et al.*, Jap. J. Appl. Phys., Pt. 1 **36** 276 (1997).
- [28] M.F. Esteban and J.M. Rojo, Thin Solid Films **15** S7 (1973).
- [29] D.W. Pashley, M.J. Stowell, M.H. Jacobs, *et al.*, Phil. Mag. **10** 127 (1964).
- [30] C.H. Lei, C.L. Jia, M. Siegert, *et al.*, Phil. Mag. Lett. **80** 371 (2000).
- [31] C.L. Jia, K. Urban, M. Mertin, *et al.*, Phil. Mag. A **77** 923 (1998).
- [32] J.D. Yu, P.F. Paradis, T. Ishikawa, *et al.*, Chem. Mater. **16** 3973 (2004).
- [33] C.L. Jia and K. Urban, Science **303** 2001 (2004).